Optimal Surrender of Guaranteed Minimum Maturity Benefits under Stochastic Volatility and Interest Rates

Boda Kang* Jonathan Ziveyi†

December 23, 2017

Abstract

In this paper we analyse how the policyholder surrender behaviour is influenced by changes in various sources of risk impacting a variable annuity (VA) contract embedded with a guaranteed minimum maturity benefit rider that can be surrendered anytime prior to maturity. We model the underlying mutual fund dynamics by combining a Heston (1993) stochastic volatility model together with a Hull and White (1990) stochastic interest rate process. The model is able to capture the smile/skew often observed on equity option markets (Grzelak and Oosterlee, 2011) as well as the influence of the interest rates on the early surrender decisions as noted from our analysis. The annuity provider charges management fees which are proportional to the level of the mutual fund as a way of funding the VA contract. To determine the optimal surrender decisions, we present the problem as a 4-dimensional free-boundary partial differential equation (PDE) which is then solved efficiently by the method of lines (MOL) approach. The MOL algorithm facilitates simultaneous computation of the prices, fair management fees, optimal surrender boundaries and hedge ratios of the variable annuity contract as part of the solution at no additional computational cost. A comprehensive analysis on the impact of various risk factors in influencing the policyholder's surrender behaviour is carried out, highlighting the significance of both stochastic volatility and interest rate parameters in influencing the policyholder's surrender behaviour. With the aid of the hedge ratios obtained from the MOL, we construct an effective dynamic hedging strategy to mitigate the provider's risk and compare different hedging performances when the policyholders' surrender behaviour is either optimal or sub-optimal.

JEL Classification: C63, G13, G22, G23
Keywords: Variable annuities, optimal surrender, GMMB, stochastic volatility, stochastic interest rates, method of lines, dynamic hedging.

*Department of Mathematics, University of York, Heslington, York, YO10 5DD, United Kingdom. Phone: +44 1904 32 4158. Email: boda.kang@york.ac.uk

†UNSW Business School, Risk and Actuarial Studies, Centre of Excellence In Population Ageing Research (CEPAR), UNSW Sydney, Sydney, NSW 2052, Australia. Phone: + 61 2 9385 8006. Email: j.ziveyi@unsw.edu.au

1 Introduction

Variable annuities (VAs) are long-dated contracts which are now dominating the market for retirement income products in most developed countries such as US, Japan and across Europe. As of June 2015, the variable annuity net assets in the US alone were in excess of $1.9 trillion, surpassing pre-Global financial crisis peaks of $1.5 trillion Holland and Simonelli (2015). A variable annuity is a binding contract between an annuity provider and policyholder where the policyholder agrees to pay a fixed premium either as a single payment or a stream of periodic payments during the accumulation phase. In return, the annuity provider undertakes to make guaranteed minimum periodic payments starting either immediately or at a deferred future date.

Variable annuities provide policyholders the flexibility to participate in the equity market while returning minimum guarantee levels in the event of poor performance of the underlying mutual fund. There are two major categories of guarantees embedded in VAs namely; guaranteed minimum death benefits (GMDBs) and guaranteed minimum living benefits (GMLBs) (see Bauer et al. (2008) and Ignatieva et al. (2016)). A GMDB is usually offered during the accumulation phase and it provides a guaranteed sum to beneficiaries in the event of untimely death of the policyholder. GMLBs offer living protection to the policyholder's income against market risk by guaranteeing a variety of benefits which can be classified as the GMxB, where "x" stands for maturity (M), income (I) and withdrawal (W). A GMMB guarantees the return of the premium payments made by the policyholder or a higher stepped-up value at the end of the accumulation period. A GMIB guarantees an income stream over an agreed period of time when the policyholder purchases a retirement annuity or annuitizes a GMMB regardless of the underlying investment performance. A GMWB guarantees the policyholder a stream of withdrawals cumulatively summing to the initial investment throughout the life of the contract conditional on the policyholder being alive.

Guarantees embedded in variable annuity contracts are usually funded by proportional fees levied from the underlying mutual fund. This paper aims to provide insights on the risks associated with trading a variable annuity contract embedded with a GMMB rider by taking the perspective of a rational policyholder who can optimally surrender the contract anytime prior to maturity.[1] Bernard et al. (2014) note that if the guarantee is deep-out-of-the-money, it may be optimal for the policyholder to surrender the contract prior to maturity as a way of avoiding paying high fees. The authors formulate the valuation problem using the geometric Brownian motion (GBM) framework and then use numerical integration techniques to analyze optimal surrender regions from the perspective of the policyholder. Such surrender behavior pose significant hazard to annuity providers' solvency, hence it is imperative to properly analyze the embedded options in VA contracts Grosen and Jorgensen (2000). As a way of discouraging policyholders from surrendering early, annuity providers normally charge penalty fees which

[1] In reality, policyholders tend to sub-optimally surrender contracts, with such decisions driven by various factors which include changes to the policyholder's financial and personal circumstances (see Bauer et al. (2015) for a detailed discussion of the underlying drivers of policyholder exercise behaviour).

takes a variety of functional forms. Bernard et al. (2014) and Shen et al. (2016) incorporate a penalty fee structure which is exponentially decreasing with time to maturity. Other penalty fee structures are discussed in Milevsky and Salisbury (2001) who denote such fees as deferred surrender charges.

Shen and Xu (2005) consider the valuation of equity-linked policies with interest rate guarantees in the presence of surrender options using the partial differential equation approach under the GBM environment. A similar problem is presented in Constabile et al. (2008) who devise a binomial tree approach to determine fair premium values. Bacinello (2013) also values participating life insurance policies with surrender options using a recursive binomial tree approach. Shen et al. (2016) take the annuity provider's perspective and use numerical quadrature techniques to derive expressions for fair management fees and the associated optimal surrender boundaries using the framework developed in Bernard et al. (2014).

The majority of the literature mentioned above has been premised under the GBM framework. Given the long-term nature of variable annuity contracts, it is crucial to accurately quantify all the major risk factors impacting the underlying fund dynamics Coleman et al. (2006); Du and Martin (2014); Kling et al. (2014). Contrary to the log-normal asset return distribution assumptions under the GBM framework Black and Scholes (1973), significant empirical studies have revealed that such distributions exhibit leptokurtic features and are characterized by heavy tails Platen and Rendek (2008). Empirical evidence also suggest that volatility of asset returns is not constant (see Christoffersen et al. (2009), Jang et al. (2014) among others). In this regard, van Haastrecht et al. (2010) highlight the importance of stochastic volatility when pricing guaranteed annuity options; contracts equivalent to GMMBs with an additional feature of converting accumulated funds into a life annuity. Kang and Meyer (2014) also note that the level of volatility of the interest rates plays a crucial role in influencing the exercise decisions of American style options prior to maturity (equivalent to surrender decisions under the current context).

Shah and Bertsimas (2010) use Monte Carlo simulation to assess the impact of both stochastic volatility and interest rates on guaranteed lifelong withdrawal benefits by making comparison with the GBM framework. The authors note that the valuations vary substantially depending on the modelling framework used. Kélani and Quittard-Pinon (2017) develop a unified valuation framework for pricing and hedging various GMLBs under the Lévy market and note that traditional modelling assumption of using the GBM framework undervalues economic capital required by providers to hedge such guarantees.

There has been less focus on the development of a realistic modelling framework for analysing the impact of various sources of risk in influencing the surrender behaviour. Such an analysis is critical to all players in the variable annuity business as it can be used as key reference when making risk management decisions. In filling this gap, the aims of this paper are twofold; the first aim involves taking the policyholder's perspective by presenting a comprehensive analysis on how the surrender behaviour is influenced by the interaction of various risk factors impacting

a VA contract embedded with a GMMB rider. In so doing, we extend the framework presented in Bernard et al. (2014) by incorporating both stochastic volatility and stochastic interest rate in our valuation framework. We assume that the policyholder's premium is invested in an underlying mutual fund which evolves under the influence of stochastic volatility Heston (1993) and stochastic interest rates Hull and White (1990).

For the second aim we take the variable annuity provider's perspective in devising a dynamic hedging algorithm for immunising the provider's net liability anytime prior to maturity of the contract. We extend the framework presented in Bernard and Kwak (2016) who consider a GMMB rider that can only be exercised at maturity when the underlying fund dynamics evolve according to the geometric Brownian motion process. There has been increasing focus on hedging of variable annuity contracts; Coleman et al. (2007) use local risk minimising strategies for hedging GMDB riders. Alonso-Garcia et al. (2017) devise a Fourier cosine based approach for pricing and hedging GMWB riders embedded in variable annuity contracts. For hedging, Alonso-Garcia et al. (2017) develop strategies that seek to minimise moment and quantile-based risk measures, such as the variance of the hedging outcomes or the 95% VaR of the hedged portfolio loss distribution. To aid our numerical analysis in this paper, we utilise the method of lines (MOL) technique Kang and Meyer (2014) as a tool for generating fair management fees, early surrender profiles and hedge ratios which are important ingredients for risk management.

The rest of the paper is structured as follows; Section 2 presents the modelling framework and formulates the corresponding value function as a free-boundary problem. Section 3 outlines the MOL approach for solving the free-boundary problem. This method generates, as part of the solution, optimal surrender profiles and the associated hedge ratios which can be used in the construction of appropriate hedging strategies. A dynamic hedging framework is presented to hedge the provider's risk in Section 4. Section 5 contains all numerical results analysing how various sources of risk influence surrender decisions and hedging performance when the policyholders surrender either optimally or sub-optimally. Concluding remarks are contained in Section 6.

2 Problem Statement

As highlighted above, we consider how the policyholder behaviour is influenced by various sources of risk impacting a VA contract embedded with a GMMB rider for the case where the contract can be surrendered anytime prior to maturity subject to penalty charges. We assume that the policyholder pays the premium as a lump sum at contract initialization which is then invested in a mutual fund consisting of units of an underlying asset, $S = (S_t)_{0\leq t\leq T}$, whose risk-neutral dynamics evolve under the influence of both stochastic volatility, $v = (v_t)_{0\leq t\leq T}$, and stochastic

interest rates, $r = (r_t)_{0\leq t\leq T}$, specified as follows[2]

$$dS_t = r_t S_t dt + \sqrt{v_t} S_t dZ_t^1, \tag{1}$$

$$dv_t = \kappa_v(\theta_v - v_t)dt + \sigma_v\sqrt{v_t}dZ_t^2, \tag{2}$$

$$dr_t = \kappa_r(\theta_r(t) - r_t)dt + \sigma_r dZ_t^3. \tag{3}$$

In the above system, $\{(Z_t^1, Z_t^2, Z_t^3); t \geq 0\}$ is a vector of correlated Wiener processes such that $\mathbb{E}_t^{\mathbb{Q}}(dZ_t^i dZ_t^j) = \rho_{ij}dt$, for $i = 1, 2$ and $j = i + 1, \cdots, 3$; v_t is the instantaneous variance which evolves according to (2) and r_t is the instantaneous risk-free interest rate which evolves according to equation (3). In equation (2), κ_v is the speed of mean reversion of the variance process to its long run mean, θ_v, and σ_v is the so-called volatility of volatility (vol-of-vol) with $\sigma_v^2 v_t$ being the variance of v_t. Likewise, κ_r is the speed of mean reversion of the interest rate process to its long run average, $\theta_r(t)$, which is time varying and σ_r is the corresponding volatility of the interest rate process. Incorporating of stochastic volatility and stochastic interest rates on the underlying asset dynamics facilitates the development of appropriate risk management strategies capable of mitigating the major sources of risks impacting VA portfolios.

In the variable annuity business, providers usually deduct various types of fees from policyholders' accounts with such fees usually expressed in layers of financial jargon. The fees typically covers ongoing costs associated with keeping the policyholder invested in the fund, transaction costs associated with buying and selling assets in the fund, and some advisory fees. In this paper, we assume a continuously compounded mutual fund fee[3] structure (see Bernard et al. (2014) and Shen et al. (2016)) such that the resulting mutual fund value from the policyholder's perspective is

$$F_t = e^{-ct} S_t, \tag{4}$$

with c being the fee expressed in percentage terms. By applying Itô's Lemma it can be shown that the risk-neutral dynamics of the fund value, $F = (F_t)_{0\leq t\leq T}$, satisfy

$$dF_t = (r_t - c)F_t dt + \sqrt{v_t} F_t dZ_t^1, \tag{5}$$

where the dynamics of v_t and r_t are as presented in equations (2) and (3), respectively.

For pricing purposes, it is more convenient to work with independent Wiener processes. The process of transforming correlated Wiener processes to independent processes is accomplished

[2]We use the Hull-White model (Hull and White, 1990) for the stochastic interest rate since it is one of the widely used short rate models in industry, however our framework and numerical algorithm can certainly handle many other short rate models, such as the Cox-Ross-Ingersoll model (Cox et al., 1985) or the Vasicek model (Vasicek, 1977).

[3]The fee structure adopted in this paper is for illustrative purposes aimed at quantifying how policyholder surrender behaviour is influenced by the level of fees applicable to the underlying fund. In practice, there are different types of fees applied to variable annuity contracts which are usually expressed in various layers of financial jargon. In addition to mutual fund management fees, there may be other third party fees payable to brokers and transaction charges whose cumulative effects may not conform with structure presented in this paper. We leave this for future research to perform empirical investigations on how to quantify all the various forms of fees applied to variable annuity contracts and the corresponding impacts of such fees to the policyholder surrender behaviour.

by applying the Cholesky decomposition such that

$$\begin{bmatrix} dZ_t^1 \\ dZ_t^2 \\ dZ_t^3 \end{bmatrix} = \begin{bmatrix} 1 & 0 & 0 \\ \rho_{12} & \sqrt{1-\rho_{12}^2} & 0 \\ \rho_{13} & \frac{\rho_{23}-\rho_{13}\rho_{12}}{\sqrt{1-\rho_{12}^2}} & \sqrt{1-\rho_{13}^2-\frac{(\rho_{23}-\rho_{13}\rho_{12})^2}{1-\rho_{12}^2}} \end{bmatrix} \begin{bmatrix} dW_t^1 \\ dW_t^2 \\ dW_t^3 \end{bmatrix},$$

where W_t^1, W_t^2 and W_t^3 are mutually independent Wiener processes.

In terms of independent Wiener processes, the fund dynamics can be re-expressed as

$$\begin{aligned} dF_t &= (r_t - c)F_t dt + \sqrt{v_t}F_t dW_t^1, \\ dv_t &= \kappa_v(\theta_v - v_t)dt + \sigma_v\rho_{12}\sqrt{v_t}dW_t^1 + \sigma_v\sqrt{1-\rho_{12}^2}\sqrt{v_t}dW_t^2, \\ dr_t &= \kappa_r(\theta_r(t) - r_t)dt + \sigma_r\left[\rho_{13}dW_t^1 + \hat{\rho}_{22}dW_t^2 + \hat{\rho}_{33}dW_t^3\right], \end{aligned}$$

where

$$\hat{\rho}_{22} = \frac{\rho_{23}-\rho_{13}\rho_{12}}{\sqrt{1-\rho_{12}^2}}, \quad \text{and} \quad \hat{\rho}_{33} = \sqrt{1-\rho_{13}^2-\frac{(\rho_{23}-\rho_{13}\rho_{12})^2}{1-\rho_{12}^2}}.$$

Using risk-neutral arguments, the value of the contract at initial time net of initial expense charges without early surrender can be represented as the expected discounted value of the terminal payout, that is

$$\mathbb{E}^{\mathbb{Q}}\left[e^{-\int_0^T r_s ds}\max(F_T, G)\right], \tag{6}$$

where F_T is the fund value at maturity time, T, with G being the guaranteed value at maturity of the contract. To avoid arbitrage opportunities, a fair insurance fee, c^*, to be charged during $t \in [0,T]$ needs to be determined such that the value in (6) is equal to the initial fund value F_0. From the expression in equation (6) when the fund value is sufficiently high relative to the guarantee level, the policyholder may find it optimal to surrender the contract early as a strategy of avoiding paying higher fees which are proportional to the fund value (see Bernard et al. (2014)). In the event of the guarantee being terminated prior to maturity, it is a common practice by annuity providers to charge penalty fees to the fund as a way of discouraging early termination of the contract such that the resulting payout to the policyholder is

$$(1-\gamma_t)F_t, \tag{7}$$

with γ_t being the penalty percentage charged for surrendering at time t. As in Bernard et al. (2014) and Shen et al. (2016), we assume that γ_t is exponentially decreasing with time and is equal to $1 - e^{-\gamma(T-t)}$ implying that if the policyholder surrenders the guarantee at $t \in [0,T]$, equation (7) becomes

$$e^{-\gamma(T-t)}F_t.$$

As outlined in Bernard et al. (2014), we will assume that the inequality $\gamma < c$ holds otherwise the contract will be held to maturity. By introducing surrender features to equation (6), the variable annuity contract can then be represented as an optimal stopping problem such that[4]

$$C(t,F,v,r) = \operatorname*{ess\,sup}_{t\leq\tau^*\leq T} \mathbb{E}^{\mathbb{Q}}\left[e^{-\int_t^{\tau^*} r_s ds} g(\tau^*, F_{\tau^*})|\mathcal{F}_t\right], \tag{8}$$

where

$$g(t,F_t) = \begin{cases} e^{-\gamma(T-t)}F_t, & t<T \\ \max(F_t,G), & t=T \end{cases}$$

and the supremum is taken over all stopping times, τ^*. Using similar arguments to those presented in Jacka (1991) and Peskir and Shiryaev (2006), the optimal stopping problem in equation (8) is equivalent to the free boundary problem

$$\begin{aligned}&\frac{\partial C}{\partial t} + (r-c)F\frac{\partial C}{\partial F} + \kappa_v(\theta_v - v)\frac{\partial C}{\partial v} + \kappa_r(\theta_r(t)-r)\frac{\partial C}{\partial r} + \frac{1}{2}vF^2\frac{\partial^2 C}{\partial F^2} + \frac{1}{2}\sigma_v^2 v\frac{\partial^2 C}{\partial v^2} \\ &+ \frac{1}{2}\sigma_r^2\frac{\partial^2 C}{\partial r^2} + \rho_{12}\sigma_v vF\frac{\partial^2 C}{\partial F\partial v} + \rho_{13}\sigma_r\sqrt{v}\frac{\partial^2 C}{\partial F\partial r} + \rho_{23}\sigma_v\sigma_r\sqrt{v}\frac{\partial^2 C}{\partial v\partial r} - rC = 0,\end{aligned} \tag{9}$$

where $0<v<\infty$, $0<r<\infty$, $0<t<T$ and $0<F<b(t,v,r)$, with $b(t,v,r)$ being the optimal surrender boundary. The PDE (9) is solved subject to boundary and terminal conditions

$$C(T,F,v,r) = \max(F,G), \tag{10}$$

$$C(t,b(t,v,r),v,r) = e^{-\gamma(T-t)}b(t,v,r), \tag{11}$$

$$\lim_{F\to b(t,v,r)}\frac{\partial C}{\partial F} = e^{-\gamma(T-t)}, \tag{12}$$

$$\lim_{F\to b(t,v,r)}\frac{\partial C}{\partial r} = 0 \quad \text{and} \quad \lim_{F\to b(t,v,r)}\frac{\partial C}{\partial v} = 0, \tag{13}$$

$$C(t,0,v,r) = G\cdot P(t,T). \tag{14}$$

Equation (10) is the payoff of the guarantee at maturity; we note that if the guarantee is held to maturity no surrender charges will be applied. The value matching condition in equation (11) guarantees the continuity of the value function at the early exercise boundary; a necessary condition enforced to avoid arbitrage opportunities. Smooth-pasting conditions in (12) and (13) are enforced in conjunction with the value matching condition to eliminate arbitrage opportunities. We handle the boundary conditions at $v=0$ and $r=0$ in a similar way as those in Kang and Meyer (2014) and Meyer (2015) with the help of the Fichera functions. Equation (14) ensuring that in the event of the fund being ruined, the policyholder will be entitled to the present value of the guarantee, where $P(t,T)$ presented in equation (15) is the zero coupon bond price when interest rate dynamics follows equation (3).

The interest rate process in (3) represents the Hull-White model Hull and White (1990). At anytime, t, the explicit solution of a zero coupon bond paying G at maturity under this framework

[4]Here for convenience, we use $C(t,F,v,r)$ to denote the value of the variable annuity contract at any time prior to maturity. We will also be writing $G \equiv G_T$ for convenience unless stated otherwise.

can be represented as

$$P(t,T) = \hat{A}(t,T)e^{-B(t,T)r_t}G, \tag{15}$$

where

$$\begin{aligned}
\hat{A}(t,T) &= A(t,T)\exp\left\{-\kappa_r \int_t^T \theta(u)B(u,T)du\right\},\\
A(t,T) &= \exp\left\{-\frac{\sigma_r^2}{2\kappa_r^2}(B(t,T)-T+t) - \frac{\sigma_r^2}{4\kappa_r}B(t,T)^2\right\},\\
B(t,T) &= \frac{1-e^{-\kappa_r(T-t)}}{\kappa_r}.
\end{aligned}$$

Once the PDE (9) is solved, the fair fee, c^*, can be determined implicitly as follows

$$c^* = \min_c\{c : F_0 = C(0, F_0^c, v_0, r_0)\}, \tag{16}$$

that is, the fair management fee at initial time is determined such that the value of the variable annuity contract is equal to the initial premium paid by the policyholder. In the next section we outline a numerical technique for solving the PDE (9) subject to terminal and boundary conditions (10)-(14). In particular, we use the method of lines technique Meyer and van der Hoek (1997) which has proved to be very powerful in solving free-boundary problems.

3 Numerical technique for determining optimal surrender features and hedge ratios

The method of lines approach is a technique that transforms a multi-dimensional PDE to a corresponding system of one-dimensional ODEs whose solution can then be readily found by using a variety of numerical methods. The method of lines techniques have found greater application in the pricing of American options. Meyer and van der Hoek (1997) consider the valuation of the standard American put option when the underlying asset is driven by the geometric Brownian motion process. Extension to the jump diffusion setting has been handled in Meyer (1998). Chiarella et al. (2009) consider the evaluation of the American call option when the underlying asset dynamics evolve under the influence of both stochastic volatility and jumps. In all these cited papers, the method of lines approach proves to be computationally efficient in terms of speed and accuracy. One major advantage of this approach is that the variable annuity (VA) contract price, delta, gamma and the early surrender boundary are all found simultaneously as part of the solution procedure at no additional computational cost.

It is more convenient to deal with the PDE with time to maturity $\tau = T - t$ instead of current

time t. Applying this transformation to the PDE (9) yields

$$\frac{\partial C}{\partial \tau} = (r-c)F\frac{\partial C}{\partial F} + \kappa_v(\theta_v - v)\frac{\partial C}{\partial v} + \kappa_r(\theta_r(t) - r)\frac{\partial C}{\partial r} + \frac{1}{2}vF^2\frac{\partial^2 C}{\partial F^2} + \frac{1}{2}\sigma_v^2 v\frac{\partial^2 C}{\partial v^2} + \frac{1}{2}\sigma_r^2\frac{\partial^2 C}{\partial r^2} + \rho_{12}\sigma_v vF\frac{\partial^2 C}{\partial F \partial v} + \rho_{13}\sigma_r\sqrt{v}\frac{\partial^2 C}{\partial F \partial r} + \rho_{23}\sigma_v\sigma_r\sqrt{v}\frac{\partial^2 C}{\partial v \partial r} - rC. \tag{17}$$

Equation (17) is solved subject to the boundary conditions specified in the system (10)-(13). In solving (17), we first discretise the partial derivative terms with respect to v, r and τ, and retain continuity in the F direction. In disretising v, we set $v_m = m\triangle v$, for $m = 0, 1, \cdots, M$. The interest rate domain is discretised such that, $r_n = n\triangle r$ for $n = 0, 1, \cdots, N$ while the time interval is partitioned into K equally spaced sub-intervals by letting $\tau_k = k\triangle\tau$ for $k = 0, 1, \cdots, K$. At any given time step, the variable annuity contract can then be represented as, $C(\tau_k, F, v_m, r_n) \equiv C^k_{m,n}(F)$. With this discretisation, the delta of the VA contract with respect to F is here denoted as

$$V(\tau_k, F, v_m, r_n) = \frac{\partial C^k_{m,n}(F)}{\partial F} \equiv V^k_{m,n}(F). \tag{18}$$

We now present finite difference approximations for the derivatives with respect to v and r. We use central difference approximations for the second order terms such that

$$\frac{\partial^2 C}{\partial v^2} = \frac{C^k_{m+1,n} - 2C^k_{m,n} + C^k_{m-1,n}}{(\Delta v)^2} \quad \text{and} \quad \frac{\partial^2 C}{\partial r^2} = \frac{C^k_{m,n+1} - 2C^k_{m,n} + C^k_{m,n-1}}{(\Delta r)^2}. \tag{19}$$

We also use a central difference approximation for the mixed partial derivative terms such that

$$\frac{\partial^2 C}{\partial F \partial v} = \frac{V^k_{m+1,n} - V^k_{m-1,n}}{2\Delta v} \quad \text{and} \quad \frac{\partial^2 C}{\partial F \partial r} = \frac{V^k_{m,n+1} - V^k_{m,n-1}}{2\Delta r}. \tag{20}$$

The cross derivative term with respect to v and r is discretised as

$$\frac{\partial^2 C}{\partial v \partial r} = \frac{C^k_{m+1,n+1} - C^k_{m-1,n+1} - C^k_{m+1,n-1} + C^k_{m-1,n-1}}{4\Delta v \Delta r}. \tag{21}$$

We discretise the first-order derivative terms with respect to v and r such that

$$\frac{\partial C}{\partial v} = \frac{C^k_{m+1,n} - C^k_{m-1,n}}{2\Delta v} \quad \text{and} \quad \frac{\partial C}{\partial r} = \frac{C^k_{m,n+1} - C^k_{m,n-1}}{2\Delta r}. \tag{22}$$

For the discretisation with respect to time, we use a first-order backward finite difference scheme for the first two time steps so that

$$\frac{\partial C}{\partial \tau} = \frac{C^k_{m,n} - C^{k-1}_{m,n}}{\Delta\tau}. \tag{23}$$

Equation (23) is only first-order accurate with respect to time, however, Meyer and van der Hoek (1997) show that the accuracy can be enhanced by considering a second-order approximation scheme. From the third time step onwards, Meyer and van der Hoek (1997) show that this is achieved by using the scheme

$$\frac{\partial C}{\partial \tau} = \frac{3}{2}\frac{C^k_{m,n} - C^{k-1}_{m,n}}{\Delta\tau} - \frac{1}{2}\frac{C^{k-1}_{m,n} - C^{k-2}_{m,n}}{\Delta\tau}, \tag{24}$$

which is a three-level quotient difference scheme. Details on how the coefficients, 3/2 and 1/2, arise can be found in Meyer (2015). We substitute the finite difference approximations in equations (18)-(24) into the PDE (17) and obtain the corresponding system of ODEs for the option delta, $V^k_{m,n}$ for $k = 0, 1, \cdots, K$, $m = 0, 1, \cdots, M$ and $n = 0, 1, \cdots, N$. For the first two time steps, the PDE is transformed to

$$\begin{aligned}
&\frac{v_m F^2}{2}\frac{d^2C^k_{m,n}}{dF^2} + \rho_{12}\sigma_v v_m F\frac{V^k_{m+1,n} - V^k_{m-1,n}}{2\Delta v} + \frac{\sigma_v^2 v_m}{2}\frac{C^k_{m+1,n} - 2C^k_{m,n} + C^k_{m-1,n}}{(\Delta v)^2} \\
&\quad + (\kappa_v\theta_v - \kappa_v v_m)\frac{C^k_{m+1,n} - C^k_{m-1,n}}{2\Delta v} + \rho_{13}\sigma_r\sqrt{v_m}F\frac{V^k_{m,n+1} - V^k_{m,n-1}}{2\Delta r} \\
&\quad + \frac{\sigma_r^2}{2}\frac{C^k_{m,n+1} - 2C^k_{m,n} + C^k_{m,n-1}}{(\Delta r)^2} + (\kappa_r\theta_r - \kappa_r r_n)\frac{C^k_{m,n+1} - C^k_{m,n-1}}{2\Delta r} \\
&\quad + \rho_{23}\sigma_v\sigma_r\sqrt{v_m}\frac{C^k_{m+1,n+1} - C^k_{m+1,n-1} - C^k_{m-1,n+1} + C^k_{m-1,n-1}}{4\Delta v\Delta r} \\
&\quad + (r_n - c)F\frac{dC^k_{m,n}}{dF} - r_n C^k_{m,n} - \frac{C^k_{m,n} - C^{k-1}_{m,n}}{\Delta\tau} = 0.
\end{aligned} \tag{25}$$

The ODE for all subsequent time steps can be shown to be

$$\begin{aligned}
&\frac{v_m F^2}{2}\frac{d^2C^k_{m,n}}{dF^2} + \rho_{12}\sigma_v v_m F\frac{V^k_{m+1,n} - V^k_{m-1,n}}{2\Delta v} + \frac{\sigma_v^2 v_m}{2}\frac{C^k_{m+1,n} - 2C^k_{m,n} + C^k_{m-1,n}}{(\Delta v)^2} \\
&\quad + (\kappa_v\theta_v - \kappa_v v_m)\frac{C^k_{m+1,n} - C^k_{m-1,n}}{2\Delta v} + \rho_{13}\sigma_r\sqrt{v_m}F\frac{V^k_{m,n+1} - V^k_{m,n-1}}{2\Delta r} \\
&\quad + \frac{\sigma_r^2}{2}\frac{C^k_{m,n+1} - 2C^k_{m,n} + C^k_{m,n-1}}{(\Delta r)^2} + (\kappa_r\theta_r - \kappa_r r_n)\frac{C^k_{m,n+1} - C^k_{m,n-1}}{2\Delta r} \\
&\quad + \rho_{23}\sigma_v\sigma_r\sqrt{v_m}\frac{C^k_{m+1,n+1} - C^k_{m+1,n-1} - C^k_{m-1,n+1} + C^k_{m-1,n-1}}{4\Delta v\Delta r} \\
&\quad + (r_n - c)F\frac{dC^k_{m,n}}{dF} - r_n C^k_{m,n} - \frac{3}{2}\frac{C^k_{m,n} - C^{k-1}_{m,n}}{\Delta\tau} - \frac{1}{2}\frac{C^{k-1}_{m,n} - C^{k-2}_{m,n}}{\Delta\tau} = 0.
\end{aligned} \tag{26}$$

After taking boundary conditions into consideration we must solve the $(M-1)\times(N-1)$ ODEs at each time step, τ_k. This process is accomplished in two steps. The first step involves re-writing the second order ODEs in equations (25) and (26) as a system of first order ODEs in the form

$$\frac{dC^k_{m,n}}{dF} = V^k_{m,n}, \tag{27}$$

$$\frac{dV^k_{m,n}}{dF} = A_{m,n}(F)C^k_{m,n} + B_{m,n}(F)V^k_{m,n} + P^k_{m,n}(F), \tag{28}$$

where $A_{m,n}(F)$, $B_{m,n}(F)$ and $P^k_{m,n}(F)$ are found by comparing (27) with (25) or (26).

The second step involves applying the Riccati transformation to equations (27) and (28). By using similar arguments as in Meyer and van der Hoek (1997) and Chiarella et al. (2009), the solution of the system (27)-(28) can be represented by the Riccati transformation

$$C^k_{m,n}(F) = R_{m,n}(F)V^k_{m,n}(F) + W^k_{m,n}(F), \tag{29}$$

where $R_{m,n}(F)$ and $W^k_{m,n}(F)$ are solutions of the initial value problems

$$\frac{dR_{m,n}}{dF} = 1 - B_{m,n}(F)R_{m,n}(F) - A_{m,n}(F)(R_{m,n}(F))^2, \quad R_{m,n}(0) = 0, \tag{30}$$

$$\frac{dW^k_{m,n}}{dF} = -A_{m,n}(F)R_{m,n}(F)W^k_{m,n}(F) - R_{m,n}(F)P^k_{m,n}(F), \quad W^k_{m,n}(0) = G \cdot P(T - \tau_k, T). \tag{31}$$

The option delta, $V^k_{m,n}(F)$ satisfies the ordinary differential equation

$$\frac{dV^k_{m,n}}{dF} = A_{m,n}(F)[R_{m,n}(F)V^k_{m,n} + W^k_{m,n}(F)] + B_{m,n}(F)V^k_{m,n} + P^k_{m,n}(F). \tag{32}$$

Equation (32) is solved subject to the boundary condition

$$V^k_{m,n}(b^k_{m,n}) = e^{-\gamma\tau_k}b^k_{m,n}, \tag{33}$$

where $F = b^k_{m,n}$ is the early surrender boundary at the grid point (τ_k, v_m, r_n). In solving the above system, we first apply the implicit trapezoidal rule[5] to equation (30) on a non-uniform grid for the F domain from $[F_{\min}, \cdots, F_{\max}]$ where $F_{\min}$ is chosen to be very small (close to zero) and $F_{\max}$ is large enough to cover the early surrender boundary region. The non-uniform grid is partitioned such that $F_{\min} < \cdots < F_{\max}$. For our numerical experiments, we will take $F_{\max}$ to be eight times the strike price due to the presence of the stochastic volatility and interest rates which have significant influence on the level of the surrender boundary.

Once equation (30) is solved, we store the results offline as this is independent of time. Having determined $R_{m,n}(F)$, we proceed to solve equation (31) for F from $F_{\max}$ to $F_{\min}$ again using the implicit trapezoidal rule. This step requires the previously calculated values of $R_{m,n}(F)$. Once $R_{m,n}(F)$ and $W^k_{m,n}(F)$ have been found, it then follows from (29) and the condition (33) that the early surrender boundary satisfies

$$e^{-\gamma\tau_k}b^k_{m,n} = R_{m,n}(b^k_{m,n}) \cdot (e^{-\gamma\tau_k}) + W^k_{m,n}(b^k_{m,n}). \tag{34}$$

As equation (34) is implicit in $b^k_{m,n}$, we need to employ root-finding algorithms to find the early surrender boundary at each grid point, (τ_k, v_m, r_n).

Once the early surrender boundary has been determined, we then solve equation (32) by sweeping backwards from $F = b^k_{m,n}$ to $F_{\min}$. Having solved equations (30)-(32) for $R_{m,n}(F)$, $W^k_{m,n}(F)$ and $V^k_{m,n}(F)$ at each grid point (τ_k, v_m, r_n), we can then substitute the resulting solutions into equation (29) to obtain the corresponding variable annuity contract value, $C^k_{m,n}(F)$.

4 Dynamic Hedging

In a variable annuity contract with early surrender features, the policyholder's behaviour is highly influential on the sustainability of the business to the provider. It is imperative for the

[5]Full details on how to implement the implicit trapezoidal rule have been documented in Meyer (2015).

annuity provider to set up appropriate hedging strategies for mitigating the risk associated with early surrender (as this may result in loss of revenue) and the possibility of the embedded guarantee ending up in-the-money. In the case of a variable annuity embedded with a GMMB rider, the annuity provider's exposure is a put option at maturity or loss of premium income associated with the contract being surrendered early. Given how critical the policyholder behaviour is on the provider, in this section we present the necessary tools which can be utilised by the annuity provider in structuring appropriate hedging strategies associated with a variable annuity contract embedded with a GMMB rider.

4.1 Net hedged loss

We extend the semi-static hedging framework presented in Bernard and Kwak (2016) who devise a strategy for hedging the net liability of a variable annuity embedded with a GMMB rider that can only be exercised at maturity. Whilst Bernard and Kwak (2016) adopt the standard geometric Brownian motion for the underlying fund dynamics, our approach is premised on a GMMB rider that can be surrendered anytime prior to maturity written on an underlying fund whose dynamics is influenced by both stochastic volatility and stochastic interest rates.

In devising our framework, we develop a dynamic hedging strategy by adopting the underlying asset dynamics presented in equation (1) and the corresponding fund value which evolves according to equation (5). Discounting of all cashflows is performed with the aid of the zero-coupon bond, $\{P(t,T)\}_{0\leq t\leq T}$, whose explicit form is presented in (15). From the provider's point of view, if the policyholder is not going to surrender the contract early, the net unhedged loss at maturity for a contract initiated at t would be

$$\begin{aligned} L &= \text{payoff to policyholder} - \text{accumulated value of collected fees} \\ &= \max(G - F_T, 0) - \int_t^T (S_u - F_u)/P(u,T)du, \end{aligned} \tag{35}$$

where we assume that the fees are collected continuously as presented in equation (4). When the policyholder optimally surrender the contract before maturity, the guarantee will be out of the money as the fund value will be greater than the guarantee level implying that the net unhedged loss is

$$\begin{aligned} L &= -\text{accumulated value of collected fees and surrender charges} \\ &= -\int_t^\tau (S_u - F_u)/P(u,\tau)du - (1 - e^{-\gamma\tau})F_\tau, \end{aligned} \tag{36}$$

with γ being the early surrender charge.

As volatility is nontradable[6], we devise a risk minimisation hedging strategy for immunising the risk associated with stochastic volatility by setting up a hedging portfolio consisting of Δ_t^S units

[6]In this paper, we focus on hedging using the underlying asset only as most variable annuity providers, unlike investment banks, have limited exposure to the derivatives markets. Poulsen et al. (2009) show that the risk

of stock S_t and Δ_t^r units of the zero coupon bond $P(t,T)$. The instantaneous mark-to-market gain at time $t+dt$ of the hedge established at time t can be represented as

$$\Delta_t^S dS_t + \Delta_t^r dP(t,T), \tag{37}$$

where Δ_t^S and Δ_t^r will be presented in the next subsection. Hence the cumulative mark-to-market gain on the hedge corresponds to the accumulated value of these gains to maturity such that

$$H = \int_t^\tau \Delta_u^S dS_u + \int_t^\tau \Delta_u^r dP(u,T), \tag{38}$$

where τ is the time at which the hedging strategy is stopped (either by early surrender or upon maturity of the contract). The net hedged profit and loss (P&L) at maturity is simply $H - L$.

4.2 Hedge ratios

In this subsection we provide the detailed derivations of both Δ_t^S and Δ_t^r used in the construction of the hedging portfolio. In the current setting, the policyholder is allowed to surrender the contract anytime prior to maturity, hence the net liability of the provider towards the policyholder at time t, denoted here as Ψ_t, is the fair value of the variable annuity minus the account value

$$\Psi_t = C(t, F_t, v_t, r_t) - F_t, \tag{39}$$

where $C(t, F_t, v_t, r_t)$ represents the fair value of the VA contract, which we defined and computed in previous sections. The delta of Ψ_t with respect to S_t is then computed as

$$\frac{\partial \Psi_t}{\partial S_t} = \frac{\partial \Psi_t}{\partial F_t}\frac{\partial F_t}{\partial S_t} = \left(\frac{\partial C}{\partial F_t} - 1\right)\frac{\partial F_t}{\partial S_t}. \tag{40}$$

From Equation (4), we know that

$$\frac{\partial F_t}{\partial S_t} = \frac{F_t}{S_t}.$$

Due to the existence of stochastic volatility, our model is incomplete, hence, based on the hedge ratio presented in Equation (40), the seller of the VA contract cannot eliminate all risk by trading the underlying stock S_t and the bond $P(t,T)$. Our main objective is therefore to deal efficiently with this risk, that is, we wish to minimize the variance of the unhedged part. Following similar arguments in Poulsen et al. (2009), instead of pure delta hedging of the fair value of the VA contract, we implement a risk minimisation hedging strategy by incorporating stochastic volatility. The following proposition provides the hedge ratios needed to accomplish this risk minimization hedging.

minimisation hedging strategies outperform the delta hedging strategies when volatility is stochastic. Note that besides risk minimisation hedging, vanilla options can as well be used to hedge risk associated with stochastic volatility and this forms part of our future research agenda.

Proposition 4.1. *Suppose at time $t < T$, a trader takes a position which is (i) long one unit of the variable annuity contract maturing at time T with payoff $g(T, F_T)$, whose value is $C(t, F_t, v_t, r_t)$, (ii) short e^{-ct} units of S_t (equivalent to short 1 unit of F_t) , (iii) short Δ_t^S units of the underlying asset S_t and (iv) short Δ_t^r units of $T-$maturity bond, $P(t,T)$. Let us denote the value of this portfolio as X_t, that is*

$$\begin{aligned} X_t &= C(t, F_t, v_t, r_t) - e^{-ct}S_t - \Delta_t^S S_t - \Delta_t^r P(t,T) = C(t, F_t, v_t, r_t) - F_t - \Delta_t^S S_t - \Delta_t^r P(t,T) \\ &= \Psi_t - \Delta_t^S S_t - \Delta_t^r P(t,T), \end{aligned}$$

then the hedging strategies below minimise the variance of dX_t:

$$\Delta_t^S = e^{-ct}\frac{\partial C(t, F_t, v_t, r_t)}{\partial F_t} + \frac{\rho_{12}\sigma_v}{S_t}\frac{\partial C(t, F_t, v_t, r_t)}{\partial v_t} - e^{-ct},\ \Delta_t^r = \frac{\partial C(t, F_t, v_t, r_t)}{\partial r_t} \Big/ \frac{\partial P(t,T)}{\partial r_t}.$$

Proof. Ito's formula yields

$$dC(t, F_t, v_t, r_t) = \cdots dt + C_F dF + C_v dv + C_r dr = \cdots dt + C_F \frac{dF}{dS} dS + C_v dv + C_r dr,$$

which implies that the the change in the value of the hedge over a small interval $[t, t+dt]$ (locally) is given by

$$dX_t = \cdots dt + dC - (\Delta_t^S + e^{-ct})dS - \Delta_t^r dP = \cdots dt + dC - (\Delta_t^S + e^{-ct})dS - \Delta_t^r \left(\cdots dt + \frac{\partial P}{\partial r} dr \right),$$

we denote $\Delta_t^{S,c} = \Delta_t^S + e^{-ct}$ and since $F_t = e^{-ct}S_t$, we have $\frac{dF}{dS} = e^{-ct}$, hence

$$dX_t = \cdots dt + (e^{-ct}C_F - \Delta_t^{S,c})dS + C_v dv + \left(C_r - \Delta_t^r \frac{\partial P}{\partial r} \right) dr. \tag{41}$$

If we choose

$$\Delta_t^r = \frac{\partial C(t, F_t, v_t, r_t)}{\partial r_t} \Big/ \frac{\partial P(t,T)}{\partial r_t},$$

the last term in Equation (41) disappears, such that

$$dX_t = \cdots dt + (e^{-ct}C_F - \Delta_t^{S,c})dS + C_v dv.$$

For the conditional variance, $\mathrm{var}_t(dX)$, the dt term vanishes such that

$$\begin{aligned} \mathrm{var}_t(dX) &= (e^{-ct}C_F - \Delta_t^{S,c})^2 \mathrm{var}_t(dS) + C_v^2 \mathrm{var}_t(dv) + 2(e^{-ct}C_F - \Delta_t^{S,c})C_v \mathrm{cov}_t(dS, dv) \\ &= [(e^{-ct}C_F - \Delta_t^{S,c})^2 v S^2 + C_v^2 \sigma_v^2 v + 2\rho_{12}\sigma_v (e^{-ct}C_F - \Delta_t^{S,c})C_v S v]dt. \end{aligned}$$

From the traders perspective a sensible choice of $\Delta_t^{S,c}$ is the one that minimizes the above variance. The first-order condition of $\mathrm{var}_t(dX)$ with respect to $\Delta_t^{S,c}$ is

$$-2(e^{-ct}C_F - \Delta_t^{S,c})vS^2 - 2\rho_{12}\sigma_v C_v S v = 0,$$

which yields

$$\Delta_t^{S,c} = e^{-ct}\frac{\partial C(t,F_t,v_t,r_t)}{\partial F_t} + \frac{\rho_{12}\sigma_v}{S_t}\frac{\partial C(t,F_t,v_t,r_t)}{\partial v_t},$$

hence

$$\Delta_t^{S} = e^{-ct}\frac{\partial C(t,F_t,v_t,r_t)}{\partial F_t} + \frac{\rho_{12}\sigma_v}{S_t}\frac{\partial C(t,F_t,v_t,r_t)}{\partial v_t} - e^{-ct}.$$

□

Remark 4.2. *: With the aid of the MOL presented in the previous section, we can easily generate* $\frac{\partial C(t,F_t,v_t,r_t)}{\partial F_t}$ *as part of solution of the free boundary problem at no additional computational cost. The ratios* $\frac{\partial C(t,F_t,v_t,r_t)}{\partial v}$ *and* $\frac{\partial C(t,F_t,v_t,r_t)}{\partial r_t}$ *can be obtained from the grid after all prices have been generated from the MOL algorithm and* $\frac{\partial P(t,T)}{\partial r_t}$ *has an explicit representation based on the bond pricing formula* (15)*.*

5 Numerical Results

Having outlined the techniques for inferring the policyholder behaviour in Section 3, in this section we perform various numerical experiments analysing the impact of model parameter changes to the surrender decisions. In the numerical experiments that follow, we use $F_0 = 100, G = 100$ and $T = 15$ years and the parameter set in Table 1 to analyse properties of the guaranteed minimum maturity benefit (GMMB) when the underlying fund dynamics evolve according to the Heston stochastic volatility model and the Hull-White stochastic interest rate process. When implementing the MOL, we set $M = 50, N = 50$ and $K = 780$, implying that there are 50 discretisations in volatility and interest rate directions, respectively and we use 780 time-steps due to long time to maturity (15 years) which corresponds a weekly computing frequency and also consistent with the hedging frequency presented in this section. We have used a total of $1,240$ points in the fund value direction when solving the ODEs in the above section.

v_t-Parameter	Value	r_t-Parameter	Value
κ_v	0.8	κ_r	0.5
θ_v	0.06	$\theta_r(t)$	$0.02 - 0.0001e^{-t}$
σ_v	0.4	σ_r	0.01
ρ_{12}	-0.5	ρ_{13}	0.2
λ_v	0	r_0	0.02
v_0	0.06		

Table 1: Parameters used for assessing policyholder behavior on the GMMB with surrender options. The first two columns contain parameters and the corresponding values of the stochastic variance process whilst the last two colums contain parameters and corresponding values of the stochastic interest rate process.

In addition to the parameter set in Table 1, we have also assumed that $\rho_{23} = 0$, which is the correlation between the stochastic volatility and the interest rate processes. This assumption is consistent with empirical findings on calibration of mutual fund portfolios under stochastic volatility and stochastic interest rates. The calibration process usually involves initially estimating the interest rate parameters separately using interest rate derivatives. Once the interest rate parameters have been found, they are then used for estimating the correlation between the interest rates and mutual fund (see van Haastrecht et al. (2010) for a detailed discussion on the calibration process).

5.1 Analysis of the impact of variance v and interest rate r on optimal surrender and fair management fees

As variable annuity contracts are usually treated as retirement income products, we consider a GMMB contract maturing in 15 years, that is, $T = 15$. Using the specifications in Table 1 the corresponding fair management fee c^* obtained by solving equation (16) is 4.74%. Figure 1 highlights the optimal surrender regions when interest rates are set at 2%. From both subplots we note that the early surrender boundary gradually increases with increasing volatility. The early surrender regions are concave functions in the time to maturity domain, slowly increasing to a maximum before rapidly decreasing to the guarantee level, G. This implies that when volatility is high, the variable annuity contract can only be surrendered optimally when the fund value is higher in comparison to the case when volatility is low. This is consistent with earlier findings in Bernard et al. (2014) who consider an equivalent problem under the geometric Brownian motion case and note that GMMBs are more valuable in a high volatile market. It is worth stating that the surrender boundary at expiry of the contract is neither a function of volatility nor interest rates as it must converge to the guarantee value. As volatility increases, the uncertainty in the performance of fund also increases resulting in high management fees which are proportional to the fund level as depicted in Table 2. From this table, we note that for given interest rate level, the management fees increases with volatility.

Next we analyse the impact of interest rates on the surrender boundary for a given level of volatility (v = 0.06 which translates to a volatility of 24.49%). Figure 2 shows the early surrender surface in (a), and the boundaries at different interest rate levels in (b). From Figure 2(a), we note that the early surrender surface is a decreasing function of interest rates, that is, as interest rates increase, the surface is shifted downwards. We also observe from Figure 2(a) that when interest rates are greater than 20%, the surface becomes almost flat implying that the optimal surrender boundary becomes less sensitive to changes in interest rates. This explains why the management fees[7] are exponentially decreasing with rising interest rates as depicted in both Table 2 and Figure 3(b).

[7]In practice, policyholders may behave sub-optimally and their surrender decisions may not necessarily be influenced by the interest rate levels only.

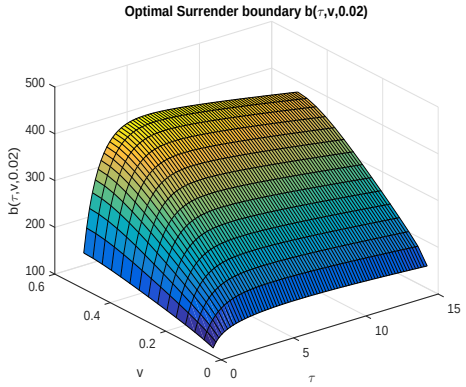

(a) Optimal surrender surface $b(\tau, v, 0.02)$.

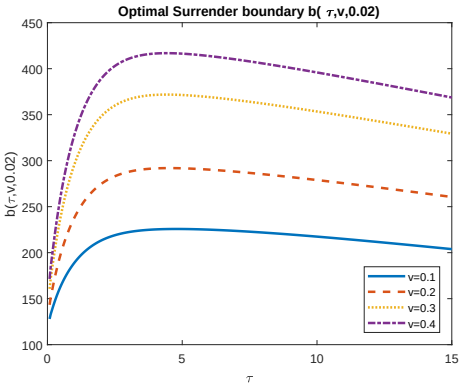

(b) Early surrender boundaries assessing the impact of stochastic volatility on optimal surrender decision.

Figure 1: Surrender region profiles for varying volatility levels when the initial interest rates are fixed at 2%. All other parameters are as presented in Table 1.

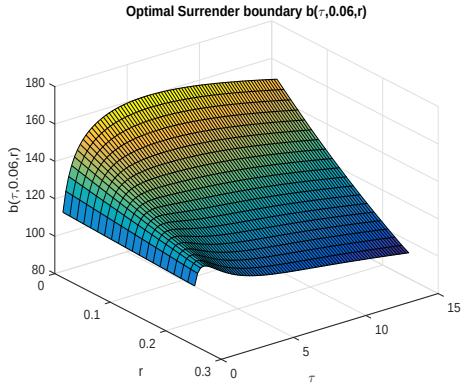

(a) Optimal surrender surface $b(\tau, 0.06, r)$.

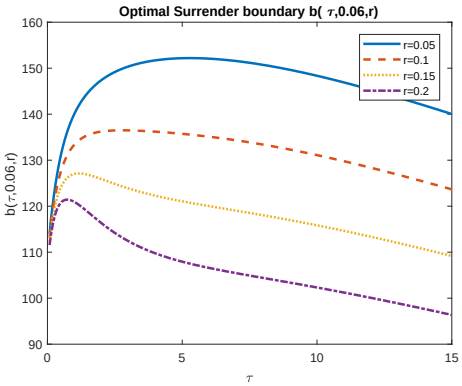

(b) Early surrender boundaries assessing the impact of interest rates on the surrender decision.

Figure 2: Surrender region profiles for varying interest rate levels when the initial fund volatility is fixed at 24.49% which corresponds to the variance of 0.06. All other parameters are as presented in Table 1.

It is of interest to assess how the optimal surrender decisions are affected jointly by changes in both interest rates and volatility. Figure 3(a) shows the early surrender surface at initial time, that is, when $\tau = 15$. The early surrender boundary is significantly increasing in the volatility domain while slowly decreasing in the interest rate domain. This implies that in a low volatility environment coupled with high interest rates, the optimality conditions for surrendering the contract early are satisfied when the fund value is much lower compared to the case where the volatility levels are high with low interest rates. However, there is not much incentive for surrendering the guarantee when the fund level is low because; (i) the fee charged on the guarantee is very low as highlighted in Table 2 and Figure 3(b), (ii) the probability of the guarantee ending up in the money is very high meaning that the policyholder stands to gain more value by delaying surrender. Conversely, a low interest rate environment with high volatility levels leads to significant fluctuations of the fund; hence higher management fees which are proportional to the fund level. It will be more sensible for the policyholder to surrender the guarantee early as a strategy of avoiding paying high management fees.

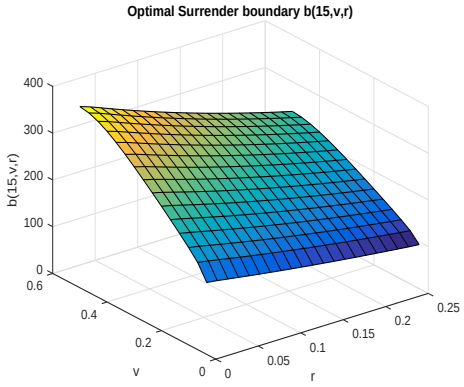

(a) Optimal surrender surface $b(15, v, r)$.

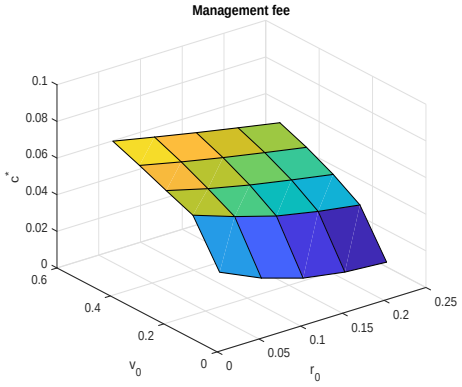

(b) Management fees at varying volatility and interest rate levels.

Figure 3: Optimal surrender region and the corresponding management fees for varying volatility and interest rate levels when $\tau = 15$. All other parameters are as presented in Table 1.

v_0 \ r_0	0.0125	0.0625	0.1125	0.1625	0.2125
0.03	0.0394	0.0292	0.0221	0.0184	0.0168
0.13	0.0629	0.0551	0.0484	0.0439	0.0404
0.23	0.0687	0.0627	0.0577	0.0534	0.0494
0.33	0.0748	0.0697	0.0650	0.0607	0.0566
0.43	0.0804	0.0756	0.0710	0.0666	0.0624

Table 2: Fair management fees, c^*, as functions of v_0 and r_0. All other parameters are as presented in Table 1.

5.2 Impact of σ_v, σ_r and the correlation coefficients on optimal surrender and the fair management fees

Another major advantage of using a more general structure for modelling the underlying fund dynamics as presented in equation (5) is the added flexibility of being able to assess how surrender behaviour is influenced by changes in underlying interest rate and volatility parameters; something which is not possible with simpler structures such as the geometric Brownian motion framework. The vol-of-vol (σ_v) and the volatility of the interest rate, σ_r, are notable drivers in influencing the dynamics of the underlying fund. Figure 4(a) shows the impact on the early surrender surfaces to changes in σ_v. In this figure, the differences are computed by subtracting the surrender boundary values generated when $\sigma_v = 20\%$ from those generated when $\sigma_v = 40\%$ for the case where the initial interest rate levels are fixed at 2%. We note that the differences are consistently positive implying that the early surrender region increases with increasing volatility of volatility, σ_v.

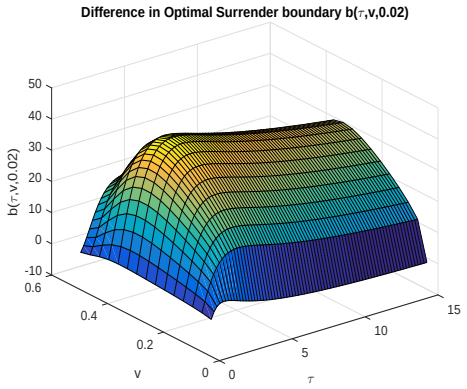

(a) Differences in optimal surrender surface, $b(\tau, v, 0.02)$, for the case where $\sigma_v = 0.4$ minus the case where $\sigma_v = 0.2$.

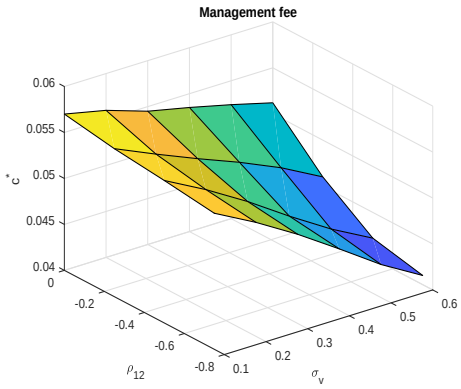

(b) Management fee when σ_v and ρ_{12} vary.

Figure 4: Assessing the impact of σ_v on the surrender region. We also infer the implications of varying σ_v and ρ_{12} on the management fees. All other parameters are as presented in Table 1.

For longer maturity contracts, an increase in σ_v generally causes a decrease in long-term volatility as revealed in Figure 5(a) which then leads to a decrease in management fees as highlighted in Figure 4(b) (see also Donnelly et al. (2014)). From Figure 4(b) we also note that the management fees increase with increases in the correlation coefficient, ρ_{12} which is the correlation between the underlying fund and the stochastic volatility process across the σ_v domain. The implied management fees to varying levels of both σ_v and ρ_{12} are also present in Table 3 for completeness.

Focusing on the impact of changes in volatility of interest rates, σ_r, on the surrender boundaries as presented in Figure 6(a) which shows the differences in surrender boundaries generated when $\sigma_r = 1\%$ minus those generated when $\sigma_r = 5\%$, we note that an increase in σ_r causes significant

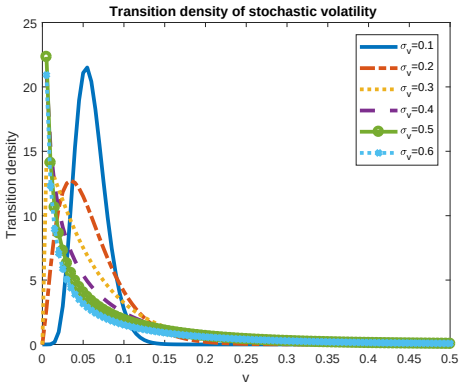

(a) Transition density of the stochastic volatility.

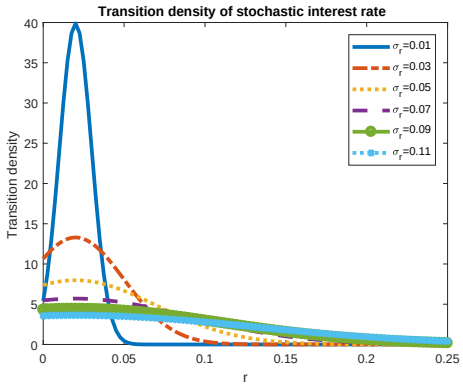

(b) Transition density of the stochastic interest rate.

Figure 5: Transition density function of SV and SI when vol-of-vol and vol of interest rate changes.

ρ_{12} \ σ_v	0.1	0.2	0.3	0.4	0.5	0.6
-0.75	0.0548	0.0524	0.0497	0.0467	0.0436	0.0410
-0.5	0.0555	0.0531	0.0504	0.0474	0.0446	0.0422
-0.25	0.0561	0.0541	0.0522	0.0504	0.0484	0.0460
0	0.0570	0.0560	0.0545	0.0535	0.0524	0.0512

Table 3: Management fee for varying ρ_{12} and σ_v. All other parameters are as presented in Table 1.

decrease of the surrender region for lower interest rates. However, as interest rates begin to rise, the surrender region becomes less sensitive to changes in σ_r. We note from Figure 5(b) that as σ_r increases, the tails of the density function becomes fatter but has less impact on the overall mean of the distribution. From equation (15), an increase in σ_r then results in higher zero coupon bond prices resulting in an increase in management fees; this behaviour is reflected in Figure 6(b) and Table 4.

From Figures 4(b) and 6(b) we observe that an increase in σ_r causes significant increase in management fees as compared to the decrease in management fees associated with increase in σ_v. For instance, when $\rho_{13} = 0$ a change of σ_r from 1% to 11% results in 63.8% increase in management fees. On the other hand when $\rho_{12} = 0$, varying σ_v from 10% to 60% results in 10.18% decrease in fees. From this analysis we can conclude that σ_r plays a very significant role in detecting the management fee structure of variable annuity contracts embedded with GMMB riders.

Another interesting finding from Figures 4(b) and 6(b) is that changes in either ρ_{12} or ρ_{13} respectively does not have significant influence on the management fee structure of these long-dated contracts. Both plots are not very sensitive to correlation coefficient changes implying that mis-specifying the correlation coefficients will not have huge impact on determination of the fair fees to be levied on such contracts.

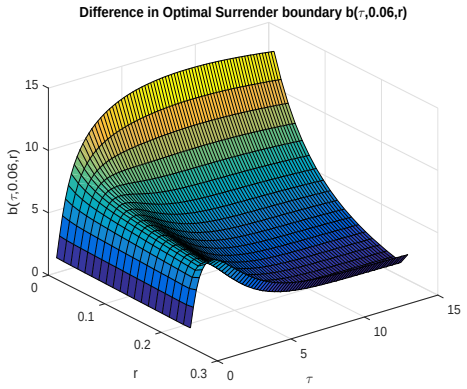

(a) Differences in optimal surrender surface, $b(\tau, 0.06, r)$, for the case where $\sigma_r = 0.01$ minus the case where $\sigma_r = 0.05$.

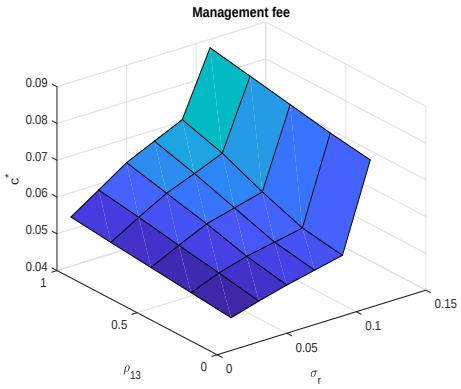

(b) Management fee when σ_r and ρ_{13} vary.

Figure 6: Assessing the impact of σ_r on the surrender region. We also infer the implications of varying σ_r and ρ_{13} on the management fees. All other parameters are as presented in Table 1.

5.3 How the penalty rate γ affects optimal surrender decisions

Due to the surrender feature in the GMMB contracts under consideration, it is of paramount importance to assess how changes in penalty fees affect the behaviour of the early surrender region. In Figure 7 we analyse how the optimal surrender region changes when the penalty fee

ρ_{13} \ σ_r	0.01	0.03	0.05	0.07	0.09	0.11
0	0.0489	0.0511	0.0531	0.0548	0.0565	0.0801
0.25	0.0500	0.0530	0.0552	0.0567	0.0582	0.0817
0.5	0.0511	0.0548	0.0583	0.0603	0.0623	0.0837
0.75	0.0522	0.0567	0.0609	0.0639	0.0671	0.0857
1	0.0534	0.0584	0.0635	0.0670	0.0705	0.0877

Table 4: Management fees for varying ρ_{13} and σ_r. All other parameters are as presented in Table 1.

is varied. Figure 7(a) considers the case where r_0 is fixed at 2% and infers the differences in the surrender region between $\gamma = 0$ and $\gamma = 0.5\%$. From this figure we note the differences increases with maturity and volatility; there is a curvature developing with maturity indicating the exponentially decreasing penalty fee structure adopted in this paper. Introducing penalty fees has an effect of shifting the surrender region up with huge differences noted when the volatility is high. The surrender region is not significantly affected by changes in penalty fees when the volatility is low as depicted from the plot. Towards maturity of the contract the differences vanishes as the boundary under both scenarios converge to the guarantee level, G, which is independent of both stochastic volatility and interest rates.

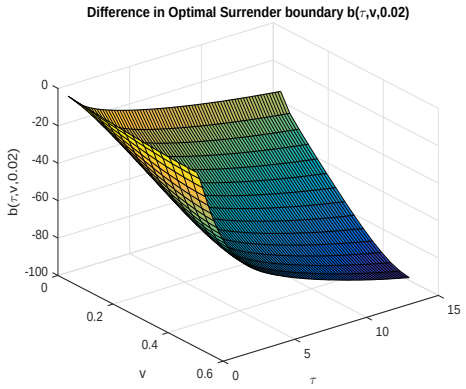

(a) Difference in optimal surrender surface, $b(\tau, v, 0.02)$, for the case when $\gamma = 0$ minus the case when $\gamma = 0.005$.

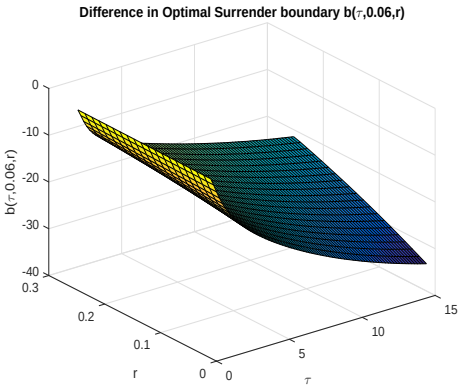

(b) Difference in Optimal surrender surface, $b(\tau, 0.06, r)$, for the case when $\gamma = 0$ minus the case when $\gamma = 0.005$.

Figure 7: Comparisons of early surrender regions for different penalty fee levels. All other parameters are as presented in Table 1.

By fixing the volatility at 24.49% (which is equivalent to the variance of 0.06) and computing the surrender boundary differences when $\gamma = 0$ and $\gamma = 0.5\%$ as presented in Figure 7(b), we note a gradual increase in the differences of the surrender region with increasing maturity across the entire interest rate domain. The differences are slightly higher for lower interest rates compared to the case when interest rates are high.

A GMMB contract which can be surrendered anytime prior to maturity as presented in equation (8) is a typical American style option. It is well known that such options are more valuable relative to their European style counterparts. It is worthwhile to assess how the values of the GMMBs with surrender options compare with those which cannot be surrendered early as presented in Figure 8. In this figure we compute the difference between the values of the European style guarantees from those with surrender features. From this graph, as expected, we note that the guarantees with surrender features are consistently more valuable than the European style guarantees. Such differences increase with increasing volatility and interest rates.

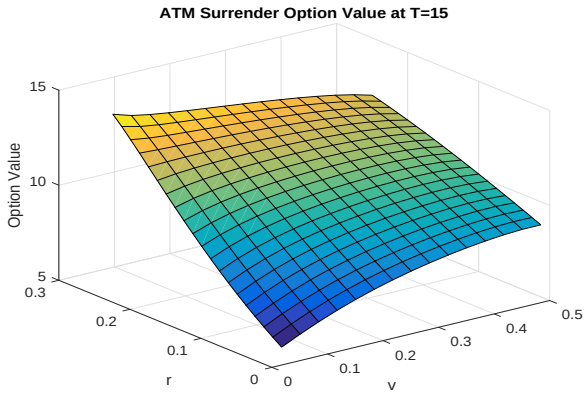

Figure 8: GMMB premium values for a contract with surrender option minus premiums for a European style GMMB. All other parameters are as presented in Table 1.

5.4 What are the hedge ratios and how much the surrender is worth?

One superior feature about the method of lines approach which we have utilised in generating the surrender boundaries is that it simultaneously compute premiums of the variable annuity contract together with the sensitivities of such premiums to changes in the underlying fund value and other state variables as part of the solution at no additional computational cost. In practice, such sensitivities are commonly referred to as "hedge ratios" with the most popular being the delta and the gamma. Figure 9 shows the delta and gamma surfaces for varying interest rates and underlying fund value when the volatility is fixed at 24.49%. From Figure 9(a) we note that deltas for at-the-money (ATM) guarantees lies between 0.7 and 0.8; with those for deep in-the-money guarantees equal to one across the entire interest rate domain. This implies that for every \$1 increase in the underlying fund value, such guarantee will as well appreciate by \$1. As the levels of interest rates increase, we note that deltas for out-of-the-money guarantees increase sharply for any given fund value. The corresponding gamma profiles at different interest rate levels are presented in Figure 9(b). Gamma is a measure of the sensitivity of the delta to changes in the underlying fund value.

To have a greater perspective on the interaction between the fund value, delta and gamma we

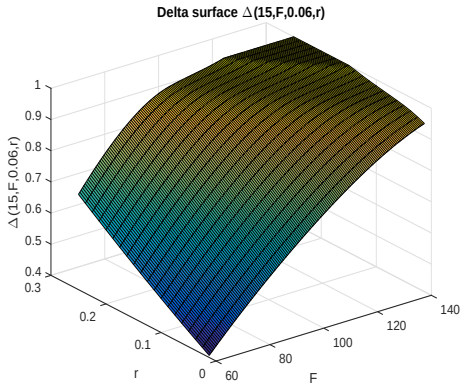

(a) Delta surface $\Delta(15, F, 0.06, r)$ for a fixed level of variance which corresponds to an underlying volatility of 24.49%.

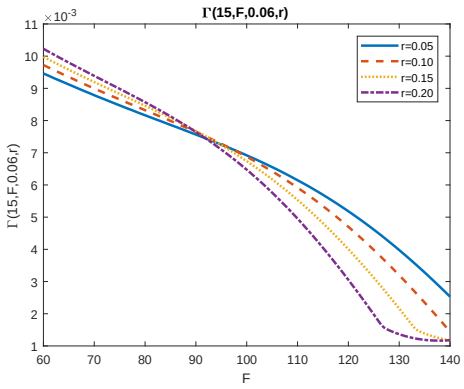

(b) Gamma plots for different levels of interest rates. We have set the variance at 0.06 and $T = 15$.

Figure 9: Hedge ratios when the variance is set at 0.06 and all other parameters as presented in Table 1.

present Table 5 which has the corresponding values for the case when the interest rates are set at 2% and volatility at 24.49%. We consider an ATM guarantee on a fund whose current value is \$100. From the table we note that the corresponding delta for an ATM guarantee is 0.6977 with a gamma of 0.006795. The corresponding value of the variable annuity contract has been found to be \$104.8758. Should the fund value go up to \$101, the policyholder can estimate that the \$100 strike contract will now be worth around \$105.5755. The new delta of this \$100 strike contract on an underlying fund whose value is now \$101 should be around 0.7045. This is obtained by simply adding the gamma of 0.006795 to the old delta of 0.6977.

F	Δ	Γ
80.0000	0.5673	0.008057
90.0000	0.6306	0.007435
100.0000	0.6977	0.006795
110.0000	0.7671	0.005937
120.0000	0.8317	0.005003

Table 5: Hedge ratios when $v = 0.06, \tau = 15$ and $r = 0.02$. All other parameters are as presented in Table 1.

We wrap up the analysis by presenting Figure 10 which assesses the impact of varying volatility on the delta and gamma profiles when interest rates are fixed at 2%. From Figure 10(a) we note that deltas for ATM contracts are close to 0.5 across the volatility domain, which are much lower than those in the interest rate domain when volatility is fixed. We also note that the gamma profiles in Figure 10(b) behave differently to those presented in Figure 9(b); this shows that volatility and interest rates have unique impacts on the underlying fund dynamics.

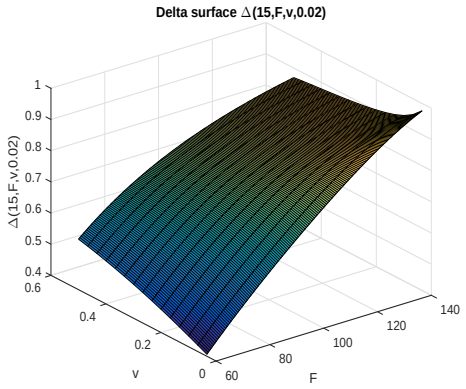

(a) Delta surface $\Delta(15, F, v, 0.02)$ for a fixed interest rate level.

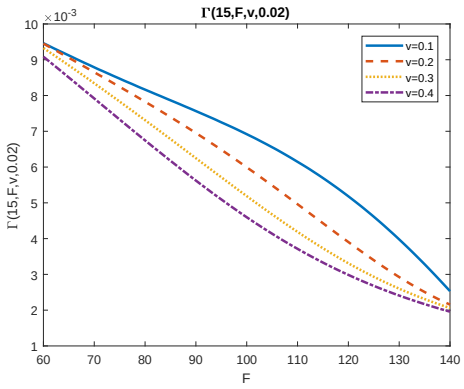

(b) Gamma plots for different levels of interest rates. We have set the initial interest rate level at 2% and a maturity of $T = 15$.

Figure 10: Hedge ratios when the initial interest rate level is set at 2% and all other parameters as presented in Table 1.

5.5 Dynamic Hedging of Net Liability

In this subsection we provide numerical illustrations on the performance of the dynamic hedging strategy presented in Section 4 where the portfolio is rebalanced on weekly basis. We adopt the parameter set presented in Table 1 in analysing how the variable annuity provider can hedge the exposures associated with the GMMB rider which can be surrendered early. The hedging strategy has been structured to mitigate the risks associated with movements of the financial variables such as the underlying stock price, volatility and interest rate on one hand and the policyholders' behaviour on the other hand.

With the aid of the quantities computed in Section 4, we implement the dynamic hedging strategy using the underlying stock and a zero coupon bond. Figure 11(a) shows the histogram (distribution) for the profit and loss (P&L) profiles of hedged and unhedged positions in the case where the policyholder optimally surrender the contract. From this figure, we note that the hedged position provide a P&L profile which is almost symmetric with a mean of 0.0768 and a standard deviation of 8.0561 as presented in Table 6. These statistics are much smaller compared to those for an unhedged position (which has a mean of -0.6416 and standard deviation of 22.1609). Hedging a rational policyholder behaviour does not bias the outcome in either direction, which highlights the effectiveness of the strategy presented in Section 4. However, in Figure 11(a) we note that the distribution of the unhedged position has more mass on the left reflecting the provider's potential losses in the event of the contract being optimally surrendered.

The potential losses are more pronounced in the event of sub-optimal surrender behaviour by the policyholder where we note a very fat tail associated with the unhedged position in Figure 11(b). From this figure, the provider has the potential of incurring a maximum loss of \$100 which corresponds to the guarantee attached to the variable annuity contract if the position

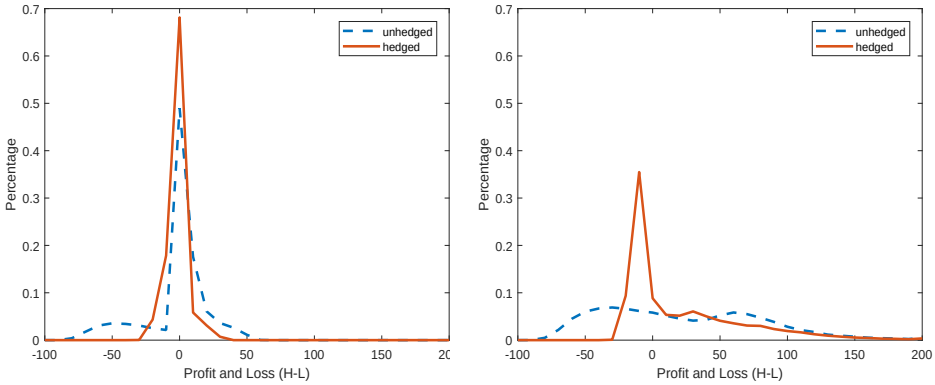

(a) Distribution if policyholder surrender optimally

(b) Distribution if policyholder surrender sub-optimally

Figure 11: Comparison of hedging when policyholder surrender optimally or sub-optimally

is unhedged. From Figure 11(b), we observe that a dynamic hedge limits the potential losses associated with sub-optimal behaviour. Sub-optimal behaviour also introduces extra uncertainty as reflected in the third column of Table 6 for both the hedged and unhedged positions which have higher means and standard deviations as compared to those associated with rational surrender behaviour. From Table 6 we note that the 95% value-at-risk (VaR) also gradually increase as the surrender behaviour drifts from optimality for both the hedged and unhedged positions.

Behaviour	$B_t = B_t^{opt}$		$B_t = 130$		$B_t = \infty$	
Hedge	Hedged	unHedged	Hedged	unHedged	Hedged	unHedged
Mean	0.0768	−0.6416	0.4819	−2.6667	22.1156	21.9517
StDev	8.0561	22.1609	9.7887	26.2778	45.4701	59.5614
95% VaR	−16.8086	−63.8897	−18.4025	−65.1529	−18.9617	−65.6169

Table 6: Statistics of the provider's net Profit and Loss (P&L), B_t is the level the policyholder choose to surrender the contract.

The last column of Table 6 corresponds to the case where the policyholder chooses not to surrender the contract early and holds it to maturity. In this case, regardless of whether it is optimal to surrender early or no, the contract is held to maturity resulting in more exposure to the provider as revealed by the associated standard deviation and VaR.

As one would expect, by comparing Figures 11(a) and 11(b) we note that a hedging strategy associated with rational policyholder behaviour is more effective than the one corresponding to sub-optimal behaviour. Also, in all the cases presented in Table 6, the hedged positions outperform the unhedged positions highlighting the importance of putting risk mitigating strategies in place. In reality, policyholders behave irrationally hence it is critical to have a deeper understanding on magnitude of risks associated with offering guarantees which can be surrendered early.

6 Conclusions

In this paper we have presented a framework for analysing how the policyholder surrender behaviour is influenced by changes in various sources of risks impacting a variable annuity (VA) contract embedded with a guaranteed minimum maturity benefit. We presented a method of lines approach that allows us to efficiently determine not only the prices but also the early optimal surrender boundaries and the hedge ratios of a VA contract when the underlying fund dynamics evolves under the influence of stochastic volatility and stochastic interest rates. Compared to the geometric Brownian motion framework where volatility is assumed to be constant, a model incorporating stochastic volatility captures "volatility smile / skew" often observed on the equity options market. Furthermore, a model incorporating stochastic interest rate is also able to capture better the optimal surrender boundary especially given that those VA contracts are long-dated. As the method of lines algorithm generates hedge ratios as part of the solution process, we have utilised such ratios in devising a dynamic hedging strategy for the net liability of the variable annuity provider.

We formulated the valuation problem of a variable annuity contract with surrender feature as a free-boundary problem which is solved with the aid of the method of lines. The fair fee which depends on model parameters has been computed after determining the value of the contract. The numerical illustrations reveal that additional to the levels of volatility and interest rates, different parameter values of the model such as vol-of-vol (σ_v), volatility of interest rate (σ_r) and the penalty rate (γ) have significant influence on the optimal surrender behaviour of the policyholder. We have performed detailed and comprehensive analysis on such effects in Section 5.

We have also inferred how the policyholder surrender behaviour affects the hedge effectiveness from the annuity provider's point of view. A key finding is that dynamic hedging strategies associated with rational policyholder behaviour outperform equivalent strategies on sub-optimal surrender behaviour. A potential line of future research will involve further analysis on how realistic policyholder behaviour patterns affect the effectiveness of hedged portfolios. It will be worthwhile to incorporate transaction costs associated with rebalancing the portfolio in analysing the effectiveness of such hedging strategies. In reality, transaction charges may be too large thus rendering the strategy impractical. Further research will assess the optimal rebalancing frequencies in the presence of transaction costs. As variable annuity contracts form part of retirement income products, it will also be worthwhile to model the valuation problem under the life-cycle consumption framework, incorporating policyholder preferences, thus, extending the work of Horneff et al. (2015).

References

J. Alonso-Garcia, O. Wood, and J. Ziveyi. Pricing and hedging guaranteed minimum withdrawal benefits under a general Lévy framework using the COS method. *Quantitative Finance*, page forthcoming, 2017.

A. R. Bacinello. Pricing Guaranteed Life Insurance Participating Policies with Annual Premiums and Surrender Option. *North American Actuarial Journal*, 7(3):1–17, 2013.

D. Bauer, A. Kling, and J. Rub. A Universal Pricing Framework for Guaranteed Minimum Benefits in Variable Annuities. *ASTIN Bulletin*, 38:621–651, 2008.

D. Bauer, J. Gao, T. Moenig, E. R. Ulm, and N. Zhu. Policyholder Exercise Behaviour in Life Insurance: The State of Affairs. *Risk Management and Insurance Faculty Publications. Paper 1. Available on: http* : $//scholarworks.gsu.edu/rmi_{f}acpub/1$, 2015.

C. Bernard and M. Kwak. Semi-static hedging of variable annuities. *Insurance: Mathematics and Economics*, 67: 173–186, 2016.

C. Bernard, A. MacKay, and M. Muehlbeyer. Optimal Surrender Policy for Variable Annuity Guaratees. *Insurance: Mathematics and Economics*, 55:116–128, 2014.

F. Black and M. Scholes. The pricing of corporate liabilities. *Journal of Political Economy*, 81:637–659, 1973.

C. Chiarella, B. Kang, G. H. Meyer, and A. Ziogas. The Evaluation of American Option prices Under Stochastic Volatility and Jump-Diffusion Dynamics Using the Method of Lines. *International Journal of Theoretical and Applied Finance*, 12(3):393–425, 2009.

P. Christoffersen, S. Heston, and K. Jacobs. The shape and term structure of the index option smirk: Why multifactor stochastic volatility models work so well. *Management Science*, 12:1914–1932, 2009.

T. Coleman, Y. Li, and M. Patron. Hedging guarantees in variable annuities under both equity and interest rate risks. *Insurance: Mathematics and Economics*, 38(2):215–228, 2006.

T. F. Coleman, Y. Kim, Y. Li, and M. Patron. Robustly hedging variable annuities with guarantees under jump and volatility risks. *Journal of Risk and Insurance*, 74(2):347–376, 2007. doi: 10.1111/j.1539-6975.2007.00216.x.

M. Constabile, I. Massabo, and E. Russo. A binomial model for valuing equity-linked policies embedding surrender options. *Insurance: Mathematics and Economics*, 42:873–886, 2008.

J. C. Cox, E. J. Ingersoll, and A. A. Ross. A theory of the term structure of interest rates. *Econometrica*, 2: 385–408, 1985.

R. Donnelly, S. Jaimungal, and D. H. Rubisov. Valuing guaranteed withdrawal benefits with stochastic interest rates and volatility. *Quantitative Finance*, 14(2):369–382, 2014.

D. Du and C. Martin. Variable Annuities-Recent Trends and the Use of Captives. *Federal Reserve Bank of Boston, available on: https* : $//www.bostonfed.org/bankinfo/publications/variable-annuities.pdf$, 2014.

A. Grosen and P. L. Jorgensen. Fair valuation of life insurance liabilities: The impact of interest rate guarantees, surrender options, and bonus policies . *Insurance: Mathematics and Economics*, 26:37–57, 2000.

L. A. Grzelak and C. Oosterlee. On the Heston Model with Stochastic Interest Rates. *SIAM Journal of Financial Mathematics*, 2:255–286, 2011.

S. L. Heston. A Closed-Form Solution for Options with Stochastic Volatility with Applications to Bonds and Currency Options. *The Review of Financial Studies*, 6(2):327–343, 1993.

D. Holland and A. Simonelli. Variable Annuity Sales Increase Sharply, VA Net Assets Approaching $2 Trillion Mark; Fixed Indexed Annuity Sales Record Second Strongest Quarter Ever. *Insured Retiment Institute Issues Second-Quarter 2015 Annuity Sales Report*, 2015.

V. Horneff, R. Maurer, O. S. Mitchell, and R. Rogalla. Optimal life cycle portfolio choice with variable annuities offering liquidity and investment downside protection. *Insurance: Mathematics and Economics*, 63:91–107, 2015.

J. Hull and A. White. Pricing interest-rate-derivative securities. *Review of Financial Studies*, 3(4):573–592, 1990.

K. Ignatieva, A. Song, and J. Ziveyi. Pricing and Hedging of Guaranteed Minimum Benefits under Regime-Switching and Stochastic Mortality. *Insurance: Mathematics and Economics*, 70:286–300, 2016.

S. D. Jacka. Optimal Stopping and American Put. *Mathematical Finance*, 1(2):1–14, 1991.

W. W. Jang, Y. H. Eom, and D. H. Kim. Empirical Performance of Alternative Option Pricing Models with Stochastic Volatility and Leverage Effects. *Asia-Pacific Journal of Financial Studies*, 14:432–464, 2014.

B. Kang and G. H. Meyer. Pricing an american call under stochastic volatility and interest rates. In R. Dieci, X. Z. He, and C. Hommes, editors, *Nonlinear Economic Dynamics and Financial Modelling: Essays in Honour of Carl Chiarella*, pages 291–314. Springer, Springer Cham Heidelberg New York Dordrecht London, 2014.

A. Kélani and F. Quittard-Pinon. Pricing and hedging variable annuities in a Lévy market: a risk management perspective . *The Journal of Risk and Insurance*, 84(1):209–238, 2017.

A. Kling, R. Ruez, and J. Rub. The Impact of Stochastic Volatility on Pricing, Hedging, and Hedge Efficiency of Withdrawal Benefit Guarantees in Variable Annuities . *European Actuarial Journal*, 4(2):281–314, 2014.

G. H. Meyer. The Numerical Valuation of Options with Underlying Jumps. *Acta Mathematica*, 47:69–82, 1998.

G. H. Meyer. The Time-Discrete Method of Lines for Options and Bonds. *World Scientific Publishing Company*, 2015.

G. H. Meyer and J. van der Hoek. The Evaluation of American Options with the Method of Lines. *Advances in Futures and Options Research*, 9:265–285, 1997.

M. Milevsky and T. Salisbury. A real option to lapse a variable annuity: can surrender charges complete the market? *Conference Proceedings of the 11th Annual International AFIR Colloquium*, 1, 2001.

G. Peskir and A. Shiryaev. *Optimal Stopping and Free Boundary Problems*. Lectures in Mathematics. ETH Zrich. Birkhuser Basel, 2006.

E. Platen and R. Rendek. Empirical Evidence on Student-t Log-Returns of Diversified World Stock Indicies. *Journal of Statistical Theory and Practice*, 2(2):233–251, 2008.

R. Poulsen, K. Reiner Schenk-Hoppé, and C.-O. Ewald. Risk minimization in stochastic volatility models: model risk and empirical performance. *Quantitative Finance*, 9(6):693–704, 2009.

P. Shah and D. Bertsimas. An Analysis of the Guaranteed Withdrawal Benefits for Life Option . *Working paper available on:* $http://ssrn.com/abstract = 1312727$, 2010.

W. Shen and H. Xu. The valuation of unit-linked policies with or without surrender options. *Insurance: Mathematics and Economics*, 36:79–92, 2005.

Y. Shen, M. Sherris, and J. Ziveyi. Valuation of guaranteed minimum maturity benefits in variable annuities with surrender options . *Insurance: Mathematics and Economics*, 69:127–137, 2016.

A. van Haastrecht, R. Plat, and A. Pelsser. Valuation of guaranteed annuity options using a stochastic volatility model for equity prices. *Insurance: Mathematics and Economics*, 47(47):266–277, 2010.

O. Vasicek. An Equilibrium characterization of the Term Structure. *Journal of Financial Economics*, 5:177–188, 1977.